Regions of Prevalence in the Coupled Restricted Three-Body Problems Approximation

Roberto Castelli *

Abstract

This work concerns the role played by a couple of the planar Circular Restricted Three-Body problem in the approximation of the Bicircular model. The comparison between the differential equations governing the dynamics leads to the definition of *Region of Prevalence* where one restricted model provides the best approximation of the four-body model. According to this prevalence, the Patched Three-Body Problem approximation is used to design first guess trajectories for a spacecraft travelling under the Sun-Earth-Moon gravitational influence.

Keywords:
Bicircular model, Coupled three-body problem approximation, Poincaré section, Regions of prevalence

Introduction

The motion of a small celestial body or of an artificial satellite is subjected to the gravitational influence of many bodies and, from a purely mathematical point of view, the restricted n-body problem should be considered in studying the dynamics. Since for $n > 2$ the problem is not integrable, the detection of trajectories in this framework is extremely difficult therefore, for applicative purposes in celestial mechanics and mission design, the approach followed so far is to produce first guess trajectories in a simplified dynamical model and then, by means of some opti-

*Institute for Industrial Mathematics, University of Paderborn, Warburger Str. 100, 33098 Paderborn, Germany and BCAM - Basque Center for Applied Mathematics, Bizkaia Technology Park, 48160 Derio, Bizkaia, Spain. (rcastelli@bcamath.org)

mization tools or multiple shooting methods, to refine them to be solutions for the complex system.

Dealing with spacecraft trajectories, the traditional approach to construct orbits between a planet and an orbiting moon is the Hohmann transfer, based on 2-body dynamics. In the work of Belbruno and Miller, [1] where the Earth-Moon gravitational system is augmented with the perturbation of the Sun, low energy transfers and ballistic capture to the Moon have been introduced with a significant reduction of fuel consumption with respect to the Hohmann transfer. The dynamical system theory that stands behind the low energy transfer is the restricted Three-Body problem (CR3BP): the invariant manifold structures related to periodic orbits provide the dynamical channels in the phase space that allow the ballistic captures of a spacecraft to the Moon.

The perturbation of the third primary, like the Sun in the Earth-Moon system, is modelled coupling together two restricted Three-Body problems: partial orbits from different restricted problems are connected into a single trajectory, yielding energy efficient transfers to the Moon [2], interplanetary transfers [3] or very complicated itineraries [4].

The procedure requires the choice of a Poincaré section where the phase spaces of the two different models have to intersect: the analysis of the Poincaré maps of the invariant manifolds reduces the design of the trajectory to the selection of a point on the section. The Poincaré section plays also a role in the accuracy of the approximation of the undertaken dynamical system: indeed the encounter with the Poincaré section is the criteria for switching from the first to the second restricted three-body problem.

Although it has been shown that the solutions in a simplified model like the CR3BP are very good approximations to real trajectories in the complicated and full system [5], this work deepens from a more theoretical point of view the role played by the two restricted three-body problems in the approximation of the 4-body system.

The undertaken model considered here for the 4-body dynamics is the Bicircular model (BCP), [6], while the two restricted problems are the Earth-Moon CR3BP and the Sun-(Earth+Moon) CR3BP, where the Sun and the Earth-Moon barycenter play the role of primaries. The comparison of the mentioned systems leads to the

definition of *Regions of Prevalence* where one of the restricted problem produces the better approximation of the Bicircular model and therefore it should be preferred in designing the trajectory.

Then, setting the Poincaré section according to this prevalence, the coupled restricted Three-Body problem approximation is implemented to design low energy transfers leaving Lyapunov orbits in the Sun-Earth system and targeting the Moon's region.

The plan of the paper is the following. In the first section the CR3BP is briefly recalled and the equations of motion for the BCP in a inertial reference frame are written. Then, in section 2, the comparison between the BCP and each one of the restricted problem is performed: this analysis enables to define, in section 3, the regions of prevalence of the two restricted systems in the approximation of the 4-body model. Section 4 concerns the design of the transfer trajectory while section 5 deepens on the numerical scheme used to analyse the intersection of the invariant manifolds and to select the connection points on the Poincaré section. Finally, in the last section, some of the results are discussed.

1. Dynamical models

Circular Restricted Three-Body problem

The CR3BP is a simplified case of the general Three Body Problem and models the motion of the massless particle under the gravitational influence of two bodies, with masses $M_1 < M_2$, that are revolving with constant angular velocity in circular orbit around their centre of mass, see [7]. In the following only the planar motion is considered.

In a rotating reference frame centered in the centre of mass, where the units of measure are normalised so that the total mass, the distance between the primaries and their angular velocities are equal to 1, the primaries are fixed on the x-axis at positions $(-\mu, 0)$ and $(1-\mu, 0)$ while the motion $z(t) = x(t) + iy(t)$ of the massless particle evolves following the differential equation

$$\frac{d^2z}{dt^2} + 2i\frac{dz}{dt} - z = -\left[\frac{(1-\mu)(z+\mu)}{\| z+\mu \|^3} + \frac{\mu(z-(1-\mu))}{\| z-(1-\mu) \|^3}\right] \tag{1}$$

where $\mu = M_2/(M_1 + M_2)$ is the mass ratio.

In (x, y) components the equation of motion assumes the form

$$\ddot{x} - 2\dot{y} = \Omega_x \ , \qquad \ddot{y} + 2\dot{x} = \Omega_y$$

where $\Omega(x, y) = (x^2 + y^2)/2 + (1 - \mu)/r_1 + \mu/r_2 + \mu(1 - \mu)/2$ is the potential function. The subscripts of Ω denote the partial derivatives, while $r_{1,2}$ are the distances between the moving particle and the primaries. The advantage to study the dynamics in a rotating frame is that system (1) is Hamiltonian and autonomous and admits a first integral called Jacobi constant

$$J(x, y, \dot{x}, \dot{y}) = -(\dot{x}^2 + \dot{y}^2) + 2\Omega(x, y) \ .$$

Therefore the phase space is foliated in 3-dimensional energy manifolds

$$E(h) = \{(x, y, \dot{x}, \dot{y}) \in R^4 \ : J(x, y, \dot{x}, \dot{y}) = h\}$$

whose projections onto the configuration space are known as Hill's regions. For any fixed value of h the Hill's regions prescribe the regions where the particle is allowed to move.

The potential Ω admits five critical points, the Lagrangian points $L_i, i = 1 \ldots 5$, and represent equilibrium points for the vector field. The points L_4 and L_5 correspond to equilateral triangle configurations, while the remaining are placed on the x-axis and correspond to collinear configurations of the masses. Of particular interest for mission design are L_1 and L_2 and the periodic orbits surrounding them that play the role of gates in the Hill's region, see for instance [8].

Bicircular model

The Bicircular model (BCP), see [9], consists in a restricted four-body problem where two of the primaries are rotating around their centre of mass, which is meanwhile rotating together with the third mass around the barycenter of the system. The massless particle is moving under the gravitational influence of the primaries and does not affect their motion. It is assumed that the motion of the primaries, as like as the motion of the test particle are co-planar. The low eccentricity of the Earth's and Moon's orbit and the small inclination of the Moon's orbital plane allow to consider the Bicircular a quite accurate model to describe the dynamics of a spacecraft in the Sun-Earth-Moon scenario; see for instance [10] and [11]. On the

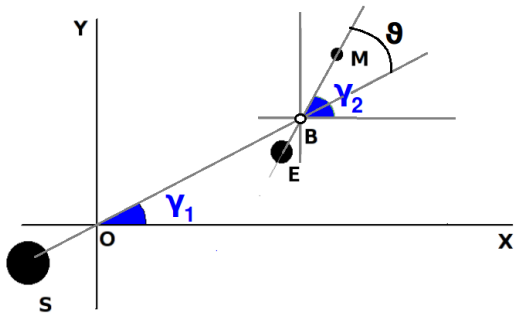

Figure 1: Positions of the primaries in inertial reference frame

other hand, it has to be remarked that the Bicircular model is not coherent since the movement of the primaries does not solve the Three-Body problem and, as a consequence, the total energy is not conserved. A more realistic model, not considered in the following of this paper, is the Quasi Bicircular model proposed and studied in [12] and [13].

Referring to Fig. 1, let S, E, M be the positions of the three primaries, namely the Sun, the Earth and the Moon while B and O indicate the Earth-Moon barycenter and the total centre of mass of the system. For a choice of time-space units of measure, let be defined the following quantities: w_1 and w_2 the angular velocities respectively of the couple S and B around O and the couple E and M around B; L_S and L_M the distances from the Sun to the point B and from the Earth to the Moon; M_m, M_e, M_s the masses of the Moon, the Earth and the Sun and G the gravitational constant. Moreover let μ_s and μ_m be the mass ratios

$$\mu_m = \frac{M_m}{M_e + M_m}, \quad \mu_s = \frac{M_e + M_m}{M_e + M_m + M_s} \ . \tag{2}$$

With respect to an inertial reference frame (X, Y) with the origin fixed in the barycenter O and where τ denotes the time coordinate, the positions of the primaries are given by

$$\begin{aligned} S &= -\mu_s L_S e^{i(\varphi_0 + w_1\tau)} \\ E &= (1-\mu_s) L_S e^{i(\varphi_0 + w_1\tau)} - \mu_m L_M e^{i(\phi_0 + w_2\tau)} \\ M &= (1-\mu_s) L_S e^{i(\varphi_0 + w_1\tau)} + (1-\mu_m) L_M e^{i(\phi_0 + w_2\tau)} \end{aligned}$$

In order to lighten the notation, in the following $\gamma_1(\tau) = \varphi_0 + w_1\tau$ and $\gamma_2(\tau) = \phi_0 + w_2\tau$ are used.

The motion $Z(\tau) = X(\tau)+iY(\tau)$ of the spacecraft, subjected to the gravitational field generated by the aforesaid system of primaries, is governed by the second order differential equation

$$\frac{d^2Z}{d\tau^2} = -G\left[\frac{M_s(Z-S)}{\parallel Z-S \parallel^3} + \frac{M_e(Z-E)}{\parallel Z-E \parallel^3} + \frac{M_m(Z-M)}{\parallel Z-M \parallel^3}\right]. \tag{3}$$

In the following sections the BCP is compared with two different restricted three-body problems: the CR3BP$_{EM}$ with the Earth and the Moon as primaries and the CR3BP$_{SE}$ where the Sun and the barycenter B with mass $M_b = M_e + M_m$ play the role of massive bodies. Three different reference frames and different units of measure are involved in the analysis: the inertial reference frame and the SE-synodical reference frame whose origin is set in the centre of mass O and the EM-synodical reference frame centered in the point B.

Change of coordinates

Following the notation previously adopted, let (X, Y, τ) be the space-time coordinates in the inertial reference frame and the small letters (x, y, t) the coordinates in the rotating systems. When necessary, in order to avoid any ambiguity, the subscripts (x_s, y_s, t_s) and (x_m, y_m, t_m) are used to distinguish the set of coordinates in the CR3BP$_{SE}$ and in the CR3BP$_{EM}$ respectively. In complex notation

$$Z := X + iY, \qquad z_m := x_m + iy_m, \qquad z_s := x_s + iy_s$$

and the relations between the inertial and the synodical coordinates are given by

$$Z = L_S z_s e^{i\gamma_1}, \qquad \tau = \tfrac{t_s}{w_1}$$
$$Z = (1-\mu_s)L_S e^{i\gamma_1} + L_M z_m e^{i\gamma_2}, \qquad \tau = \tfrac{t_m}{w_2}\ .$$

Concerning with the two synodical systems, the time coordinates t_s and t_m satisfy

$$t_s = \frac{w_1}{w_2} t_m$$

while the formula for the coordinates change between (x_s, y_s) and (x_m, y_m) depends on the mutual position of the primaries. Let θ be defined as the angle between the positive x_s-semiaxis and the positive x_m-semiaxis, see Fig. 1:

$$\theta(\tau) := \gamma_2 - \gamma_1 = \theta_0 + (w_2 - w_1)\tau\ .$$

For any value of θ, the position $z_{(\cdot)}$ and the velocity $\frac{dz_{(\cdot)}}{dt_{(\cdot)}}$ of a particle in the two different synodical systems satisfy the relations

$$\begin{array}{c} z_m = \frac{L_S}{L_M} e^{-i\theta}\Big(z_s - (1-\mu_s)\Big) \\ \frac{dz_m}{dt_m} = \frac{L_S}{L_M}\frac{w_1}{w_2} e^{-i\theta}\Big[i\Big(1-\frac{w_2}{w_1}\Big)(z_s-(1-\mu_s)) + \frac{dz_s}{dt_s}\Big] \end{array} \tag{4}$$

and

$$\begin{array}{c} z_s = \frac{L_M}{L_S} e^{i\theta} z_m + (1-\mu_s) \\ \frac{dz_s}{dt_s} = \frac{L_M}{L_S}\frac{w_2}{w_1} e^{i\theta}\Big[i\Big(1-\frac{w_1}{w_2}\Big)(z_m) + \frac{dz_m}{dt_m}\Big] \ . \end{array}$$

A second differentiation provides the relations between the accelerations in the two systems:

$$\frac{d^2 z_s}{dt_s^2} = \ \frac{L_M}{L_S}\left(\frac{w_2}{w_1}\right)^2 e^{i\theta}\left[-\Big(1-\frac{w_1}{w_2}\Big)^2 z_m + 2i\Big(1-\frac{w_1}{w_2}\Big)\frac{dz_m}{dt_m} + \frac{d^2 z_m}{dt_m^2}\right] \ . \tag{5}$$

The dependence of the previous formulas on the angular velocities w_i is redundant: combining the equalities, consequence of the third Kepler's law,

$$w_1^2 L_S^3 = G(M_s + M_e + M_m),\ w_2^2 L_M^3 = G(M_e + M_m) \tag{6}$$

it follows

$$\frac{w_1}{w_2} = \left(\frac{(M_s+M_e+M_m)}{(M_e+M_m)}\frac{L_M^3}{L_S^3}\right)^{\frac{1}{2}} = \left(\frac{1}{\mu_s}\frac{L_M^3}{L_S^3}\right)^{\frac{1}{2}} \ .$$

In this work the physical parameters adopted for the numerical simulations are set according with the Jet Propulsion Laboratory ephemeris (available on-line at http://ssd.jpl.nasa.gov/?constants). In particular the mass ratios are

$$\mu_s = 3.040423402066 \cdot 10^{-6}, \quad \mu_m = 0.012150581$$

being the masses of the bodies

$$M_s = 1.988924 \cdot 10^{30} \text{ kg} \quad M_e = 5.973712 \cdot 10^{24} \text{ kg } M_m = 7.347686 \cdot 10^{22} \text{ kg} \ .$$

In the inertial reference frame, where the space coordinates are expressed in km and the time in second, the distances L_S and L_M are equal to

$$L_S = 149597870 \text{ km}\,,\ L_M = 384400 \text{ km}$$

while the values of the angular velocities w_1 and w_2 are

$$w_1 = 1.99098898 \cdot 10^{-7}\ \frac{\text{rad}}{\text{s}}, \quad w_2 = 2.6653174179 \cdot 10^{-6}\ \frac{\text{rad}}{\text{s}}.$$

2. The comparison of the BCP with the CR3BPs

The distance between the Bicircular model and each one of the CR3BP is estimated as the norm of the difference of the accelerations governing their dynamics, once they are written in the same reference frame and in the same units of measure. The comparison is carried out in the synodical frame proper of the considered restricted problem, while the units of measure in both the cases will be the dimensional ones.

Comparison with CR3BP$_{SE}$

To write the equation of motion for the BCP in SE-synodical frame only a rotation has to be applied to the inertial coordinates: $Z = \bar{z}e^{i\gamma_1}$, where $\bar{z} = z_s L_S$. In this setting the positions of the primaries are given by

$$\begin{aligned}
\bar{S} &= -\mu_s L_S \\
\bar{E} &= (1-\mu_s)L_S - \mu_m L_M e^{i(\gamma_2-\gamma_1)} \\
\bar{M} &= (1-\mu_s)L_S + (1-\mu_m)L_M e^{i(\gamma_2-\gamma_1)}.
\end{aligned}$$

The second derivative of $Z(\tau)$ turns into

$$\frac{d^2Z}{d\tau^2} = \left(\frac{d^2\bar{z}}{d\tau^2} + 2iw_1\frac{d\bar{z}}{d\tau} - w_1^2\bar{z}\right)e^{i\gamma_1}$$

then, substituting the new variables into (3), we infer

$$\frac{d^2\bar{z}}{d\tau^2} + 2iw_1\frac{d\bar{z}}{d\tau} - w_1^2\bar{z} = -G\left[\frac{M_s(\bar{z}-\bar{S})}{\parallel \bar{z}-\bar{S} \parallel^3} + \frac{M_e\big(\bar{z}-\bar{E}\big)}{\parallel \bar{z}-\bar{E} \parallel^3} + \frac{M_m(\bar{z}-\bar{M})}{\parallel \bar{z}-\bar{M} \parallel^3}\right]. \qquad (7)$$

In the same time-space system of coordinates, the equation of motion for the CR3BP$_{SE}$ is

$$\frac{d^2\bar{z}}{d\tau^2} + 2iw_1\frac{d\bar{z}}{d\tau} - w_1^2\bar{z} = -G\left[\frac{M_s(\bar{z}-\bar{S})}{\parallel \bar{z}-\bar{S} \parallel^3} + \frac{M_b(\bar{z}-\bar{B})}{\parallel \bar{z}-\bar{B} \parallel^3}\right].$$

It follows the difference between the two models

$$\Delta_{SE}(\bar{z}) = \parallel BCP - CR3BP_{SE} \parallel \qquad (8)$$

$$= G\Big|\Big| - \frac{M_e(\bar{z}-\bar{E})}{\parallel \bar{z}-\bar{E} \parallel^3} - \frac{M_m(\bar{z}-\bar{M})}{\parallel \bar{z}-\bar{M} \parallel^3} + \frac{M_b(\bar{z}-\bar{B})}{\parallel \bar{z}-\bar{B} \parallel^3}\Big|\Big|.$$

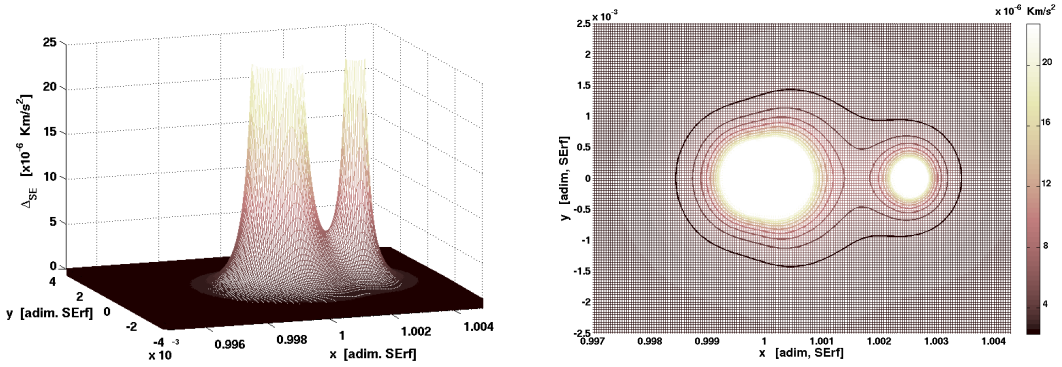

Figure 2: Level curves of Δ_{SE} for $\theta = 0$

The gap between the two models arises from the fact that in the restricted three-body problem the Earth-Moon system is considered as a unique body concentrated in its centre of mass instead of a binary system.

Relation (8) blows up in three points: the centres of the Earth and the Moon and in the barycenter B. But since the point B is placed inside the Earth and it makes sense to evaluate the error only outside the Earth's and Moon's surface, the graphic of Δ_{SE} looks like the union of two almost circular spikes around the bodies. As shown in Fig. 2, where the value of Δ_{SE} is plotted for $\theta = 0$, the error rapidly decreases to zero as the evaluation point is out of two disks around the primaries. For any different mutual position of the three primaries the picture of Δ_{SE} is different but self-similar up to rotation around the point B.

Comparison with the CR3BP$_{EM}$

Following the same procedure as before, the distance between the CR3BP$_{EM}$ and the BCP is achieved. Again, let $\bar{z}$ be used to denote the complex coordinates in a rotating reference frame and dimensional units of measure. Reminding that the origin of the EM-synodical frame is in the barycenter B that is revolving around the centre of mass O, the inertial coordinate Z and $\bar{z}$ are linked by the formula

$$Z = B + \bar{z}e^{i\gamma_2} \ , \qquad B = (1-\mu_s)L_S e^{i\gamma_1} \ .$$

The positions of the primaries

$$\begin{aligned}\bar{S} &= (S-B)e^{-i\gamma_2} = -L_S e^{i(\gamma_1-\gamma_2)}\\ \bar{E} &= (E-B)e^{-i\gamma_2} = -\mu_m L_M\\ \bar{M} &= (M-B)e^{-i\gamma_2} = (1-\mu_m)L_M\end{aligned}$$

and the acceleration of the particle

$$\frac{d^2Z}{d\tau^2} = \left(\frac{d^2\bar{z}}{d\tau^2} + 2iw_2\frac{d\bar{z}}{d\tau} - w_2^2\bar{z} - w_1^2(1-\mu_s)L_S e^{i(\gamma_1-\gamma_2)}\right)e^{i\gamma_2}$$

yield the differential equation for the BCP in dimensional EM-synodical coordinates (commonly denoted in the literature as the Sun perturbed Earth-Moon CR3BP)

$$\begin{aligned}&\frac{d^2\bar{z}}{d\tau^2} + 2iw_2\frac{d\bar{z}}{d\tau} - w_2^2\bar{z} - w_1^2(1-\mu_s)L_S e^{i(\gamma_1-\gamma_2)} =\\ &-G\left[\frac{M_s(\bar{z}-\bar{S})}{\parallel \bar{z}-\bar{S}\parallel^3} + \frac{M_e(\bar{z}-\bar{E})}{\parallel \bar{z}-\bar{E}\parallel^3} + \frac{M_m(\bar{z}-\bar{M})}{\parallel \bar{z}-\bar{M}\parallel^3}\right].\end{aligned} \tag{9}$$

The term $-w_1^2(1-\mu_s)L_S e^{i(\gamma_1-\gamma_2)}$ represents the centrifugal acceleration of B or, equivalently, the gravitational influence of the Sun on the Earth-Moon barycenter, indeed (2) and (6) imply $(1-\mu_s)w_1^2 = \frac{GM_s}{L_S^3}$. The difference between (9) and

$$\frac{d^2\bar{z}}{d\tau^2} + 2iw_2\frac{d\bar{z}}{d\tau} - w_2^2\bar{z} = -G\left[\frac{M_e(\bar{z}-\bar{E})}{\parallel \bar{z}-\bar{E}\parallel^3} + \frac{M_m(\bar{z}-\bar{M})}{\parallel \bar{z}-\bar{M}\parallel^3}\right]$$

that governs the motion in the EM restricted problem, gives the distance between the two models

$$\Delta_{EM}(\bar{z}) = \parallel BCP - CR3BP_{EM}\parallel = GM_s\left|\left|\frac{(\bar{S}-\bar{z})}{\parallel \bar{z}-\bar{S}\parallel^3} - \frac{(\bar{S}-\bar{B})}{\parallel \bar{S}-\bar{B}\parallel^3}\right|\right|.$$

The error originates because in the CR3BP$_{EM}$ the influence of the Sun on the spacecraft is considered as the same influence that the Sun produces on the centre B of the rotating frame. Indeed the error vanishes whenever the spacecraft is placed in the origin of the reference frame and grows when it moves away, see Fig. 3.

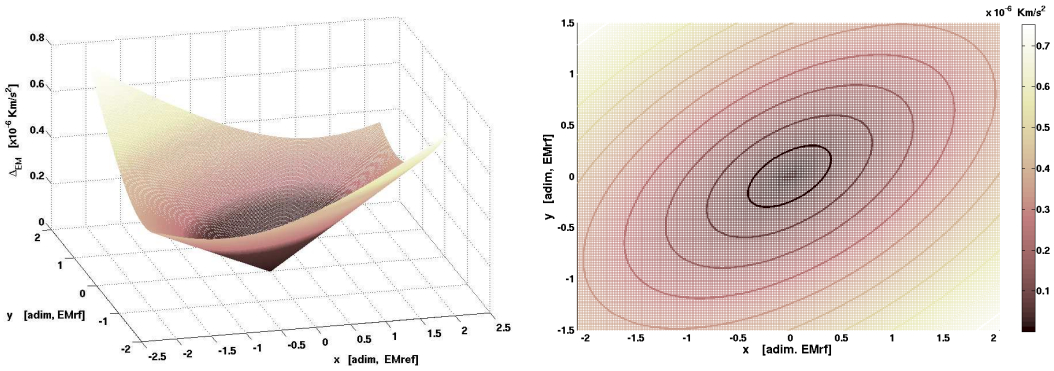

Figure 3: Level curves of Δ_{EM} for $\theta = \pi/3$

3. Regions of Prevalence

The analysis carried out in the previous section and the values obtained for the errors Δ_{SE} and Δ_{EM} confirm what one expects about the accuracy of the restricted problems in the approximation of the Bicircular model: far from the region where the Earth and the Moon are placed, the force of the Sun is predominant and the CR3BP$_{SE}$ is the appropriate model to describe the dynamics, while in the vicinity of the Earth and the Moon the CR3BP$_{EM}$ better reproduces the force field. Moreover, as shown in Fig. 4, both the errors are really small: indeed out of a disk of 10^5 km around the Earth and $3 \cdot 10^3$ km around the Moon the value of Δ_{SE} is less than $0.03\ m/s^2$, while the $\Delta_{EM} < 0.2 \cdot 10^{-3} m/s^2$ inside a disk of $1.5 \cdot 10^6$ km around the Earth.

On the other side it has to be remarked that, although the residual acceleration Δ_{EM} is small in the neighbourhood of the Earth-Moon L_1 and L_2 Lagrangian points, due to resonances the dynamics in the restricted three-body model could be considerably different from the one of a restricted four-body problem, like the Bicircular or the Quasi-Bicircular, [13, 12].

In the following the two quantities $\Delta_{SE}(z)$ and $\Delta_{EM}(z)$ are compared to define the regions where each restricted model produces the best approximation of the

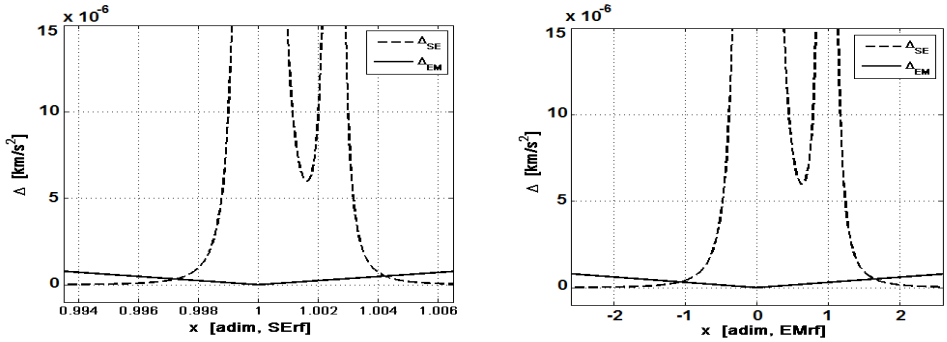

Figure 4: Profile of Δ_{SE} and Δ_{EM}, for $\theta = 0$, along the Sun-Earth-Moon line. The units of the x-axis are the adimensional Sun-Earth (left) and adimensional Earth-Moon (right).

BCP. Once a system of coordinates is chosen, let us define the function

$$\begin{aligned}\Delta E(z) &= (\Delta_{SE} - \Delta_{EM})(z) \\ &= G\left|\left| -\frac{M_e(z-E)}{\|z-E\|^3} - \frac{M_m(z-M)}{\|z-M\|^3} + \frac{M_b(z-B)}{\|z-B\|^3}\right|\right| - GM_s\left|\left|\frac{(S-z)}{\|z-S\|^3} - \frac{(S-B)}{\|S-B\|^3}\right|\right| .\end{aligned}$$

In any point z one of the restricted models has to be preferred according with the sign of ΔE: in particular where $\Delta E < 0$ the CR3BP$_{SE}$ provides a better approximation of the BCP, otherwise the CR3BP$_{EM}$.

Denote with $\Gamma(\theta)$ the zero level set of the function ΔE for a given angle θ:

$$\Gamma(\theta) := \{(x, y) : \Delta E(x + iy) = 0\} .$$

Numerical simulations show that $\Gamma(\theta)$ is a closed simple curve: we refer to the two regions bounded by $\Gamma(\theta)$ as the *Regions of Prevalence* of the two restricted problems. In the bounded region $\Delta_{EM} < \Delta_{SE}$, while in the exterior region the opposite holds. Substituting the coordinates giving the positions of the primaries, the zero level curve $\Gamma(\theta)$ is computed in SE and EM-synodical coordinates.

In Fig. 5 the zero level set of ΔE is drawn for different choices of the angle θ and in different systems of coordinates. For any angle θ the Earth, the Moon as like as the L_1 and L_2 Lagrangian points related to the CR3BP$_{EM}$ belong to the EM region of prevalence, while the CR3BP$_{SE}$ Lagrangian points are placed in the exterior region. This behavior suggests to consider the coupled CR3BP approximation for design spacecraft trajectories as discussed in the next sections.

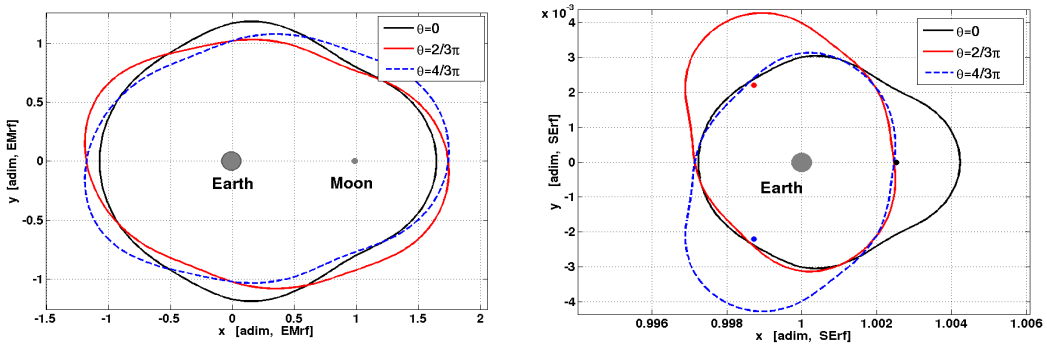

Figure 5: $\Gamma(\theta)$ with $\theta = 0, 2/3\pi, 4/3\pi$ in SE and EM reference frame

4. The coupled CR3BP approximation

The coupled CR3BP concerns the approximation of the four-body problem with the superposition of two circular restricted three-body problems, [2]. The invariant manifold structures related to periodic orbits provide dynamical channels in the phase space that enable natural transfers from and to the smaller primary. Then patching together on a suitable Poincaré section the portions of trajectory evaluated in the different models, the design of the mission is accomplished. Commonly, the Poincaré section is chosen *a priori* as a line passing through one of the massive bodies, [2], [11], [3] or lying on the coordinate axes, [8] or as boundary of the sphere of influence of one of the primaries as in [5].

Fig. 6 shows a Earth-to-Moon transfer designed in the coupled CR3BP approximation obtained exploiting the intersection between the internal unstable manifold leaving a Lyapunov orbit around L_2 in the SE system and the external stable manifold related to a Lyapunov orbit surrounding L_2 in the EM system. The Poincaré section was chosen as an hyperplane passing through the Earth and with slope of $\pi/4$ with respect the Sun-Earth line and $\pi/8$ with respect the Earth-Moon line at the crossing time.

According with the regions of prevalence previously defined, in this work the Poincaré section is defined as the hypersurface

$$PS(\theta) = \{(x, y, \dot{x}, \dot{y}) : (x, y) \in \Gamma(\theta)\}$$

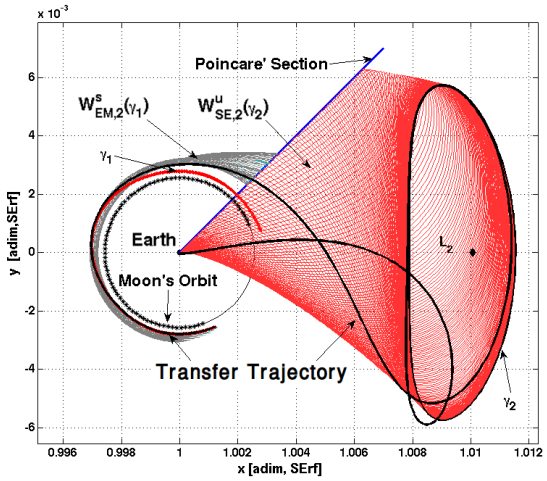

Figure 6: Trajectory in the Coupled CR3BP Approximation, in SE rotating reference frame

set on the curve $\Gamma(\theta)$ and the design of trajectories leaving a Lyapunov orbit around L_1 and L_2 in the CR3BP$_{SE}$ and directed to the vicinity of the Moon is considered. Therefore, denoting with $W^{(u),s}_{(SE),EM,i}(\gamma)$ any (un)-stable manifold related to Lyapunov orbits γ around L_i in the (SE) or EM restricted problem, the intersections of $W^s_{EM,2}(\gamma_1)$ with $W^u_{SE,1}(\gamma_2)$ and $W^u_{SE,2}(\gamma_2)$ on the surface $PS(\theta)$ need to be exploited.

Denoting with $\Theta = \left\{\theta_k = k\frac{2\pi}{K},\, k = 0, \ldots, K-1\right\}$ a set of K equispaced values in $[0, 2\pi)$, the procedure to design the transfer trajectory is the following. First an angle $\theta \in \Theta$ is chosen and the curve $\Gamma(\theta)$ in both the synodical systems is drawn. Then let γ_1 be a Lyapunov orbit around L_2 in the Earth-Moon model with Jacobi constant J_{EM} and γ_2, γ_3 a couple of Lyapunov orbits, respectively around L_2 and L_1 equilibrium points, in the Sun-Earth model with Jacobi constant J_{SE}. Compute the exterior branch of $W^s_{EM,2}(\gamma_1)$ and the interior branches of $W^u_{SE,2}(\gamma_2)$ and $W^u_{SE,1}(\gamma_3)$ until the section $PS(\theta)$ is eventually encountered.

The resulting Poincaré maps, i.e. the sets $P_W(\theta)$ of intersections between the manifold W and the Poincaré section

$$P_W(\theta) = \{(x, y, \dot{x}, \dot{y}) \in W : (x, y) \in \Gamma(\theta)\},$$

are then transformed into the same coordinate system, being θ the relative phase of the primaries. Note that since the Jacobi constant is preserved along the invariant manifolds, one of the velocity coordinates, say $\dot{y}$, is determined once $x, y, \dot{x}$ are known.

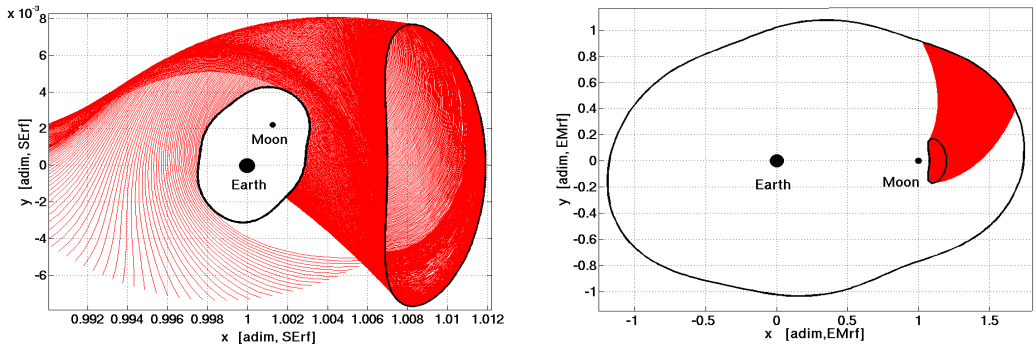

(a) (b)

Figure 7: Intersection of $W^u_{SE,2}(\gamma_2)$ and $W^s_{EM,2}(\gamma_1)$ with $\Gamma(\pi/3)$

As it appears in Fig.7(b), for almost every Lyapunov orbits around L_2 in the Earth-Moon system and every θ, the external branch of the stable manifold $W^s = W^s_{EM,2}(\gamma_1)$ invests completely the Poincaré section, yielding a Poincaré map $P_{W^s}(\theta)$ topologically equivalent to a circle, see Fig.8(a). Denote with $\mathcal{B}$ the region of the surface $PS(\theta) \cap \{J(x, y, \dot{x}, \dot{y}) = J_{EM}\}$ bounded by $P_{W^s}(\theta)$.

Looking at the projection of the curve $P_{W^s}(\theta)$ onto the $(x, \dot{x})$ plane as in Fig. 8(c), the elements $(x_B, y_B, \dot{x}_B, \dot{y}_B)$ of $\mathcal{B}$ are identified by the points $(x_B, \dot{x}_B)$ in the grey region, while y_B is obtained as solution of $(x_B, y_B) \in \Gamma(\theta)$ and $\dot{y}_B$ from the energy relation $J(x_B, y_B, \dot{x}_B, \dot{y}_B) = J_{EM}$.

Since the invariant manifolds act as separatrices in the constant energy manifolds, the points of $\mathcal{B}$ correspond to initial data for orbits transiting in the Moon's region. Therefore, for our purpose, the sets $Int = (\mathcal{B} \cap W^u_{SE,2}(\gamma_2))$ and $Int = (\mathcal{B} \cap W^u_{SE,1}(\gamma_3))$ need to be detected. Indeed, patching together the trajectories obtained integrating any point $p \in Int$ backward in time in the CR3BP$_{SE}$ and forward in the CR3BP$_{EM}$, one obtains an orbit that, starting from the SE-Lyapunov, after have passed through the EM Lyapunov gateway, will approach the Moon. Note that the above intersec-

tions are done in configuration space, thus no manoeuvre is required to join the two legs of trajectory. Moreover the angle θ is the relative phase of the primaries at the moment the trajectory intersects the curve $\Gamma(\theta)$.

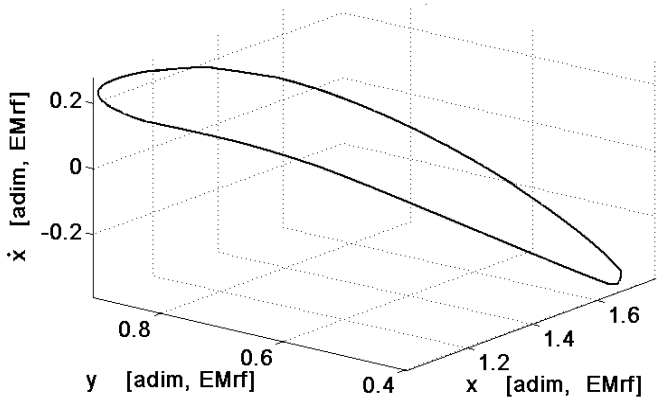

(a)

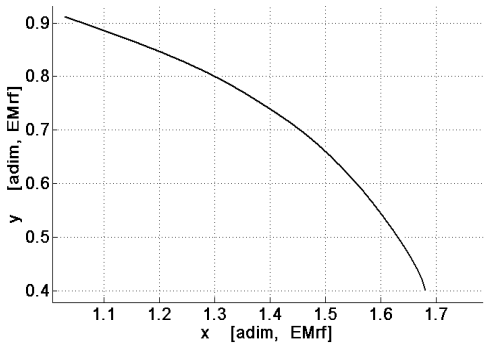

(b)

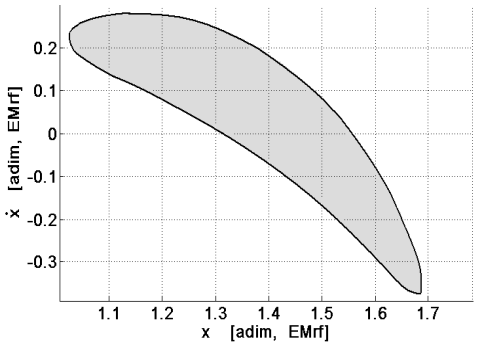

(c)

Figure 8: The intersection of $W^s_{EM,2}(\gamma_1)$ with the Poincaré section $PS(\theta)$ is a closed curve in the phase space. (a) Projection of the Poincaré map onto the $(x, y, \dot{x})$ space. (b) Projection onto the (x, y) plane. (c) In grey the projection of the region $\mathcal{B}$ onto the $(x, \dot{x})$ plane.

5. The box covering approach

This section deals with the technique used to detect the set Int of connecting points on the Poincaré section.

To begin with, the intersection of the stable manifold relative to a Lyapunov orbit in the EM system with the curve $\Gamma(\theta)$ is performed. The invariant manifolds are computed following the classical scheme based on the eigenvectors of the monodromy matrix, while the *Hénon's trick*, [14], is implemented in finding the intersections. Using the software package GAIO (Global Analysis of Invariant Objects), see [15], the four-dimensional Poincaré map is covered with box structures. A N-dimensional box $B(C, R)$ is identified by a centre $C = (C_1, C_2, \ldots, C_N) \in \mathcal{R}^N$ and a vector of radii $R = (r_1, r_2, \ldots, r_N)$ and it is defined as

$$B(C,R) = \bigcap_{i=1}^{N} \{(x_1, x_2, \ldots, x_N) \in \mathcal{R}^N \ : \ |x_i - C_i| < r_i\}.$$

Given a box B_0, two smaller sub-boxes B_1^1 B_1^2 are defined with the first radius equal to $r_1/2$ and with the property $B_1^1 \cup B_1^2 = B_0$. Continuing this process of multiple subdivision of the existing boxes along one of the radii, a larger set of smaller boxes is created with the property to cover the first box B_0. The *depth* of a family of boxes denotes the number of times the subdivision of boxes is done, starting from B_0. Any time the subdivision process is performed the number of boxes increase twofold, then the total number of boxes at the $depth = d$ is exactly 2^d. Once the family $\mathcal{F}(d)$ of boxes at a certain depth d is created, the Poincaré map of the manifold is therein inserted: only those boxes of $\mathcal{F}(d)$ containing at least one point of the Poincaré map are considered, the others are neglected, see Fig. 9(a).

Denote with $\mathcal{P}$ the family of boxes used for the covering of the Poincaré map. In order to detect the sets Int, the interior region $\mathcal{B}$ needs to be covered as well, see Fig. 9(b). The definition of the centres of the boxes used to cover $\mathcal{B}$ is made 'by columns': from the set of boxes in $\mathcal{P}$ whose centers have the same (x, y)-coordinates, let be selected the two boxes with the maximal v_{max} and minimal v_{min} value of the $\dot{x}$-coordinate. Then a new set of centres $\{C_k = (x, y, \dot{x}_k, \dot{y}_k)\}_{k=1}^{K}$ is defined, where $\dot{x}_k = v_{min} + k\Delta v$ and w_k is obtained from the Jacobi constant. Here Δv is twice the radius in the $\dot{x}$-direction of the covering boxes and $K = (v_{max} - v_{min})/\Delta v$.

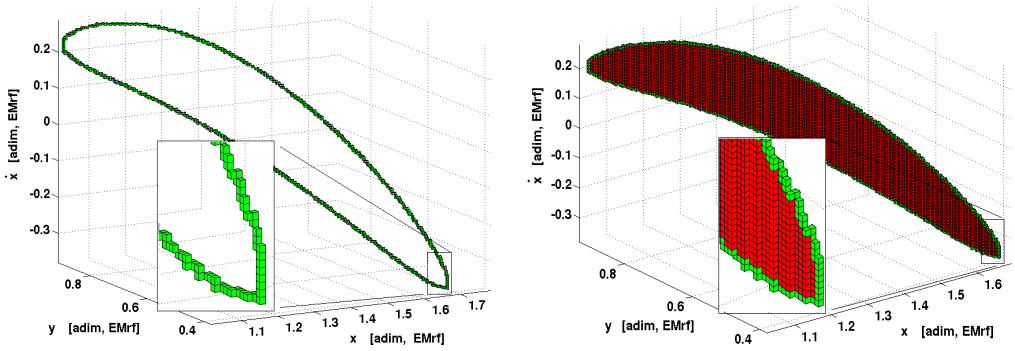

(a) (b)

Figure 9: Box covering of the Poincaré map of $W^s_{EM,2}$

In the presented simulation the covering is performed at $d = 32$: depending on the size of the Poincaré map the radii of the covering boxes result to be in the range $[4 \cdot 10^{-4}, 2 \cdot 10^{-3}]$ EM units.

Then, for a value of the Jacobi integral in the SE system, the Poincaré map of $W^u_{SE,1}(\gamma_3)$ or $W^u_{SE,2}(\gamma_2)$ is computed and, using (4), it is transformed in EM synodical coordinates, being θ the angle between the primaries. Finally, all those points of the SE Poincaré map lying in one of the boxes covering $\mathcal{B}$ are considered as transfer points.

6. Some results

The existence of connection points is tested starting from a database of 60 Lyapunov orbits in the CR3BP$_{SE}$ both around L_1 and L_2 and 60 Lyapunov orbits around L_2 in the CR3BP$_{EM}$. The Jacobi constant varies in the range $[3.0004, 3.00084]$ for the SE system and in the interval $[3.053, 3.177]$ for the EM system and 32 values of $\theta \in [0, 2\pi)$ have been considered.

From a theoretical point of view, for a choice of the parameters (θ, J_{EM}, J_{SE}) the set of intersection between the region $\mathcal{B}$ and the unstable manifolds in the Sun-Earth system may be empty, contain one or many different points.

As shown in the previous section, in the numerical approach the region $\mathcal{B}$ is replaced by its box covering, therefore the number of possible connecting points

found in the simulation depends on the size of the covering boxes and on how accurate the invariant manifolds are computed. In the presented simulations no more than three points have been found in each set Int.

Fig. 10 represents schematically the results obtained: every dark sign marks the existence of at least a point in the intersection $\mathcal{B} \cap W^u_{SE,1}$ and $\mathcal{B} \cap W^u_{SE,2}$, i.e. $\Delta V = 0$ connections. The coordinates represent the Jacobi constant of the connection point respectively in the SE and EM system and the angle θ of the Poincaré section $\Gamma(\theta)$ where the connection is detected.

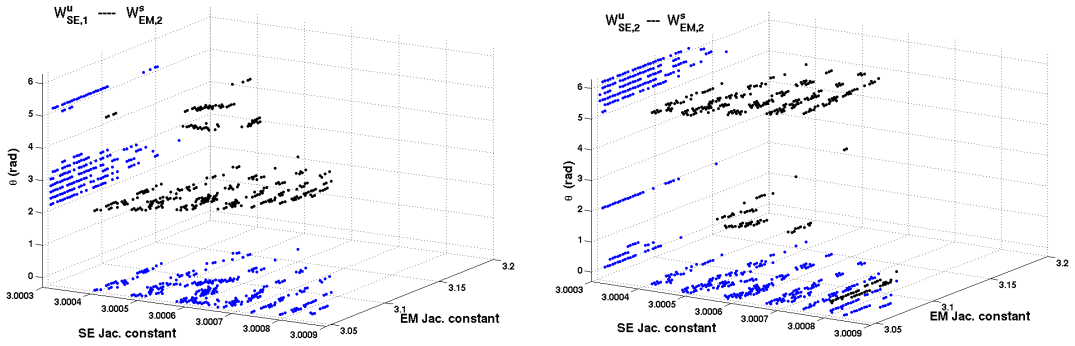

Figure 10: Zero ΔV connections between $W^u_{SE,1}$ and $W^s_{EM,2}$ (Left) and between $W^u_{SE,2}$ and $W^s_{EM,2}$ (Right)

The lighter points are the projections of the previous ones onto the SE/EM Jacobi constant plane and EM Jacobi constant/angle θ plane. In both the cases the intersections are concentrated in a range of angle θ around π and 2π respectively. This behavior is easily explained looking at the geometry of the manifold tubes emanating from the Lyapunov orbits in the two systems.

Starting from one intersection, backward and forward integration in the two CR3BP produce the complete transfer: in the following figures the darker and the lighter lines concern the pieces of trajectory integrated in the CR3BP$_{SE}$ and in the CR3BP$_{EM}$ respectively.

If no differently specified, all the evaluations are done in the SE-synodical frame and in SE-units of measure: relations (7) and (5) provide the accelerations of the spacecraft moving according to the Bicircular motion and CR3BP. According with

the notation adopted before, $\Delta_{SE}(t)$ and $\Delta_{EM}(t)$ are the norm of the difference between the instantaneous acceleration of the spacecraft provided by the restricted model along the trajectory and the acceleration that would be applied to the probe if the bicircular model has been considered.

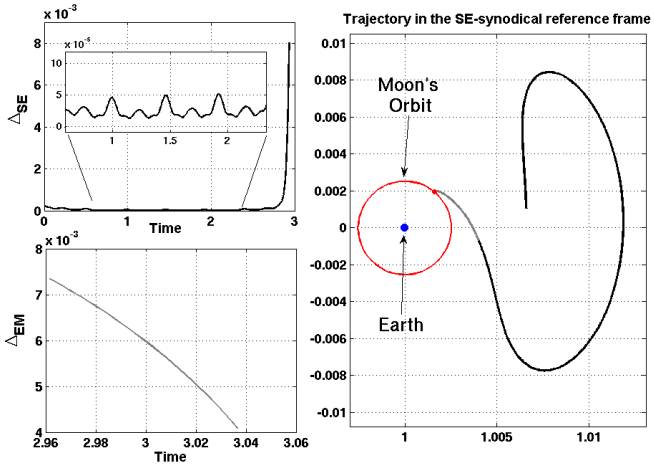

Figure 11: Example of transfer trajectory and related errors Δ_{SE}, Δ_{EM}

The bigger picture in Fig. 11 depicts the orbit in SE-synodical coordinates, from a Lyapunov orbit around L_2 to the Moon region, while the smaller ones show the values of $\Delta_{SE}(t)$ and $\Delta_{EM}(t)$.

For a given trajectory, let us consider the integral

$$\text{Total } \Delta V = \int_{t_0}^{t_c} \Delta_{SE}(t)dt + \int_{t_c}^{t_{fin}} \Delta_{EM}(t)dt$$

where t_0 is the last time the spacecraft is far from the Earth more than 2.5 times the Earth-Moon distance, t_{fin} is the first moment the spacecraft is 10000 km close to the Moon, while t_c denotes the instant when the Poincaré section is crossed.

While the function $\Delta_{EM}(t)$ and $\Delta_{SE}(t)$ measure the instantaneous and local distance between the different dynamical models, Total ΔV is regarded as the global distance between the coupled CR3BP approximation and the BCP along a trajectory. Aiming to emphasise the benefit gained choosing as Poincaré section the curve

$\Gamma(\theta)$ instead of the classical one, the above integration should be evaluated on a large number of transfers. Indeed, due to the dependence on the nominal trajectory, Total ΔV can not be considered as a measure of the accuracy of the approximating technique, but only as a statistical indicator once a certain number of tests are given.

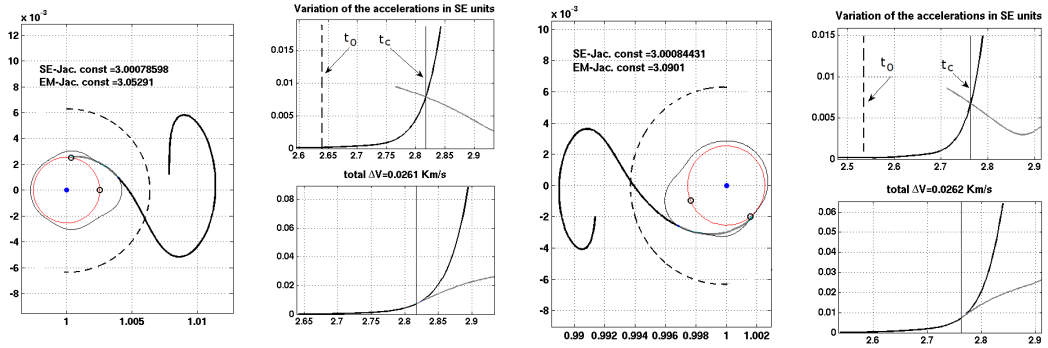

Figure 12: Two samples of trajectories designed according with the Regions of Prevalence and analysis of the residual accelerations.

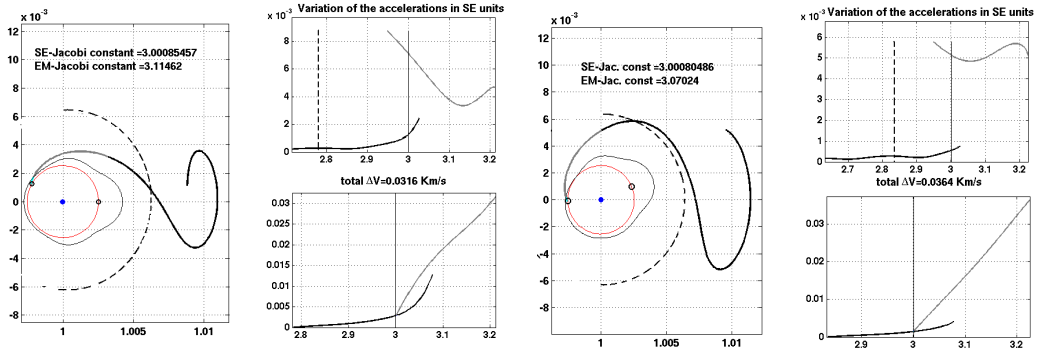

Figure 13: Two sample of trajectories designed setting the Poincaré section on lines passing through the Earth and analysis of the residual accelerations

Referring to Fig. 12, in the bigger box the dotted line remarks the circle inside which the above integration starts, the black circles show the position of the Moon when the spacecraft is on the section and the end of the travel. The black line denotes the Poincaré section at the crossing time. In the upper of the smaller figures the

values of Δ_{EM} and Δ_{SE} are plotted together, while the last graph shows the value of the integration. Starting from t_0 the error Δ_{SE} is integrated until the crossing time t_c, then the error Δ_{EM} is considered till the final time t_{fin} (lighter line) or again Δ_{SE} is integrated for a short interval of time (darker line).

Two samples of the same analysis performed on trajectories obtained coupling the two CR3BPs with a different Poincaré section are shown in Fig 13. More precisely, on the left case, the section is set on a line passing through the Earth with a slope of $\pi/4$ with respect to the Sun-Earth line and the relative phase of the Moon at the connection instant is $\theta = 0$, while on the right the unstable manifold in the SE system is cut on $x = 1 - \mu_s$ and the Moon performs an angle of $\pi/8$ with respect the Sun-Earth line when the spacecraft is on the section.

It can be noticed that the classical Poincaré section are not optimal in minimizing the residual instantaneous acceleration between the restricted models and the 4-body model: in both the cases at the crossing time the Sun-Earth is much better than the Earth-Moon restricted problem in approximating the Bicircular model. Concerning the Total ΔV indicator, the samples here proposed show a gain of around 25% of total ΔV if $\Gamma(\theta)$ is considered. Nevertheless, even in the classical setting, the value of Total ΔV evaluated along the trajectories designed in the coupled CR3BP approximation is very small compared with the flight time, from 25 to 50 m/s spread on an interval of time of $23 - 30$ days. This confirms the validity of the coupled CR3BP approximation in space mission design.

7. Conclusions

In this work the coupling of two CR3BPs has been considered in the approximation of the bicircular model. Aiming to increase the accuracy of the approximation, the dynamics in two restricted three-body models and in the bicircular one has been analysed and the regions of prevalence where each restricted model provides the best approximation of the four-body system have been defined. Then, according to these regions and by means of box-covering numerical methods, samples of trajectories leaving Lyapunov orbits in the Sun-Earth system and directed to the Moon's region have been designed. It results that these trajectories could exhibit a significant reduction of the overall residual acceleration in comparison with transfers obtained in

the traditional coupled CRTBP approximation.

Acknowledgements

The author has been supported by the Marie Curie Actions Research and Training Network AstroNet, Contract Grant No. MCRTN-CT-2006-035151.

References

[1] E. Belbruno and J. Miller. Sun-perturbed Earth-to-Moon transfer with ballistic capture. *Journal of Guidance Control and Dynamics*, 16, 1993.

[2] W. S. Koon, M. W. Lo, J. E. Marsden, and S. D. Ross. Low energy transfer to the Moon. *Celestial Mech. Dynam. Astronom.*, 81(1-2):63–73, 2001.

[3] M. Dellnitz, O. Junge, M. Post, and B. Thiere. On target for Venus—set oriented computation of energy efficient low thrust trajectories. *Celestial Mech. Dynam. Astronom.*, 95(1-4):357–370, 2006.

[4] G. Gómez, W.S. Koon, M.W. Lo, J.E. Marsden, J. Masdemont, and S.D. Ross. Connecting orbits and invariant manifolds in the spatial restricted three-body problem. *Nonlinearity*, 17:1571–1606, 2004.

[5] J.S. Parker. Families of low-energy lunar halo transfer. *Proceedings of the AAS/AIAA Space Flight Mechanics Meeting*, pages 483–502, 2006.

[6] C. Simó, G. Gómez, À Jorba, and J. Masdemont. The bicircular model near the triangular libration points of the rtbp. In *From Newton to chaos*, volume 336 of *NATO Adv. Sci. Inst. Ser. B Phys.*, pages 343–370. 1995.

[7] V. Szebehely. *Theory of orbits, the restricted problem of three bodies*. Academic Press, New York and London, 1967.

[8] W. S. Koon, M. W. Lo, J. E. Marsden, and S. D. Ross. Heteroclinic connections between periodic orbits and resonance transitions in celestial mechanics. *Chaos*, 10(2):427–469, 2000.

[9] J. Cronin, P. B. Richards, and L. H. Russell. Some periodic solutions of a four-body problem. *Icarus*, 3(5-6):423 – 428, 1964.

[10] K. Yagasaki. Sun-perturbed Earth-to-Moon transfers with low energy and moderate flight time. *Celestial Mech. Dynam. Astronom.*, 90(3-4):197–212, 2004.

[11] G. Mingotti, F.Topputo, and F. Bernelli-Zazzera. Low-energy, low-thrust transfers to the Moon. *Celestial Mech. Dynam. Astronom.*, 105(1-3):61–74, 2009.

[12] M. A. Andreu. Dynamics in the center manifold around L_2 in the quasi-bicircular problem. *Celestial Mech. Dynam. Astronom.*, 84(2):105–133, 2002.

[13] M. A. Andreu. The quasi-bicircular problem. *Ph. D. Thesis, Dept. Matemàtica Aplicada i Anàlisi, Universitat de Barcelona*, 1998.

[14] M. Hénon. On the numerical computation of Poincaré maps. *Phys. D*, 5(2-3): 412–414, 1982.

[15] M. Dellnitz, G. Froyland, and O. Junge. The algorithms behind gaio - set oriented numerical methods for dynamical systems. In *In Ergodic theory, analysis, and efficient simulation of dynamical systems*, pages 145–174. Springer, 2000.